

Polarimetric Information for Multi-Modal 6D Pose Estimation of Photometrically Challenging Objects with Limited Data

Patrick Ruhkamp^{1,2} Daoyi Gao¹ HyunJun Jung¹ Nassir Navab¹ Benjamin Busam^{1,2}

¹ TU Munich, ² 3Dwe.ai

p.ruhkamp {...} b.busam@tum.de

Abstract

6D pose estimation pipelines that rely on RGB-only or RGB-D data show limitations for photometrically challenging objects with e.g. textureless surfaces, reflections or transparency. A supervised learning-based method utilising complementary polarisation information as input modality is proposed to overcome such limitations. This supervised approach is then extended to a self-supervised paradigm by leveraging physical characteristics of polarised light, thus eliminating the need for annotated real data. The methods achieve significant advancements in pose estimation by leveraging geometric information from polarised light and incorporating shape priors and invertible physical constraints.

1. Introduction

We address limitations of 6D object pose estimation using depth sensor data affected by inaccuracies from artifacts like multi-path interference, ambient light, and transparency [24]. Utilising polarised light’s geometric information for pose estimation has shown promising results, outperforming RGB-only and RGB-D methods [9]. However, obtaining extensive annotated datasets is challenging [27, 15]. We investigate the effectiveness of polarimetric data in improving 6D object pose estimation through supervised learning. Additionally, we propose a physics-induced polarimetric self-supervision scheme to alleviate the need for large annotated real datasets [10].

2. Related Work

Polarimetric Imaging. Early studies on shape from polarisation (SfP) focus on estimating surface normals and depth information by analysing the relationship between polarisation and object surfaces. However, these works mainly operate in controlled lab environments [3, 11, 22, 29]. Monocular polarisation images are commonly used, but SfP can also utilise multiple views for depth estimation [2, 6]. Po-

larimetric images are combined with photometric information from stereo [1] or monocular RGB [31] to enhance depth predictions. Additionally, polarised light improves noisy depth maps obtained from other sensors [16]. Recent work by Ba et al. [4] employs neural networks to predict surface normals by leveraging plausible cues extracted from polarimetric images, demonstrating the disambiguation capability of such cues in SfP. Inspired by these findings, our approach incorporates shape priors from physical properties extracted from polarised light to complement pose estimation.

6D Object Pose Estimation. Dense correspondence-based methods have gained popularity for 6D object pose estimation [30, 13, 17, 19, 21]. These methods involve training neural networks to predict 2D-3D correspondences between object pixels and their corresponding 3D locations on the object’s surface. The correspondences are then used with PnP+RANSAC, the Umeyama algorithm, or direct regression to compute the 6D object pose. Zebra-Pose [23] introduces hierarchical feature representations, and zero-shot methods are being explored for 6D pose estimation [20]. However, many correspondence-based methods suffer from computationally expensive post-processing steps in RANSAC-based pose solvers. GDR-Net [26] and its follower SO-Pose [7] address this limitation by employing learning-based MLP networks to directly predict the tar-

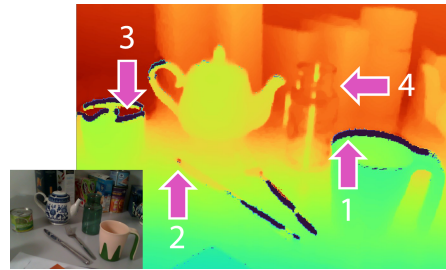


Figure 1. **Challenges in Depth Estimation for Household Objects.** Reflective boundaries (1,3) and strong reflections (2,3) cause depth miscalculations, while semi-transparent objects (4) become partially invisible to the depth sensor.

get pose from dense correspondences, thereby improving computational efficiency. In our work, we build upon these findings to directly regress the object pose.

Geometric Depth Information. Several methods, including FFB6D [12], Uni6D [14], ESA6D [18], FS6D [28], and DGEEN [5], incorporate depth information into their prediction pipelines. However, these approaches heavily rely on depth quality, which is problematic for photometrically challenging objects [9]. Geometric cues derived from polarization can potentially mitigate these issues.

Polarimetric 6D Pose Prediction. Recently published annotated datasets for real-world polarimetric category-level [27] and instance-level [9] 6D pose estimation enable the study of methods using this unexplored imaging modality. PPP-Net [9] investigates the advantages of using polarisation for object pose estimation and proposes a hybrid pipeline that combines physical model cues with learning. Unlike previous methods such as Self6D [25] and Self6D++ [24], we leverage polarimetric images and an extended differentiable renderer to incorporate geometric representations and enable self-supervision based on our invertible physical model.

3. Polarimetric Physical Model

RGB-D sensors often rely on active illumination for depth measurement. However, they are susceptible to photometric challenges such as translucency and reflections, leading to erroneous depth estimates. Figure 1 demonstrates such depth artifacts. We instead leverage the surface normals obtained from polarisation for 6D object pose estimation, where accurate 3D information is crucial. When unpolarised light passes through a linear polariser or is reflected at Brewster’s angle from a surface, it becomes polarised. The combination of specular and diffuse reflection results in a partially polarised reflected light, which carries information about the surface properties. We propose to use surface normals obtained from polarisation to overcome the photometric challenges faced by RGB-D sensors.

Image Formation Model. The polarisation image formation model [8] considers the degree of polarization (DoP) ρ and angle of polarisation (AoP) ϕ of the incoming light. By analysing the oscillation state of light captured by polarisation filters at different angles φ_{pol} , the polarised intensities can be computed using: $I_{\varphi_{pol}} = I_{un} \cdot (1 + \rho \cos(2(\phi - \varphi_{pol})))$. We find φ and ρ from the over-determined system of linear equations using linear least squares. Depending on the surface properties, AoP is calculated as:

$$\begin{cases} \phi_d[\pi] = \alpha & \text{for diffuse reflection} \\ \phi_s[\pi] = \alpha - \frac{\pi}{2} & \text{for specular reflection,} \end{cases} \quad (1)$$

where $[\pi]$ indicates the π -ambiguity and α is the azimuth angle of the surface normal \mathbf{n} . We can further relate the

viewing angle $\theta \in [0, \pi/2]$ to the degree of polarisation by considering Fresnel coefficients, thus DoP is similarly given by [3]

$$\begin{cases} \rho_d = \frac{(\eta-1/\eta)^2 \sin^2(\theta)}{2+2\eta^2-(\eta+1/\eta)^2 \sin^2(\theta)+4\cos(\theta)\sqrt{\eta^2-\sin^2(\theta)}} \\ \rho_s = \frac{2\sin^2(\theta)\cos(\theta)\sqrt{\eta^2-\sin^2(\theta)}}{\eta^2-\sin^2(\theta)-\eta^2\sin^2(\theta)+2\sin^4(\theta)}, \end{cases} \quad (2)$$

with the refractive index of the observed object material η . Solving equation 2 for θ , we retrieve three solutions $\theta_d, \theta_{s1}, \theta_{s2}$, one for the diffuse case and two for the specular case. For each of the cases, we can now find the 3D orientation of the surface by calculating the surface normals $\mathbf{n} = (\cos \alpha \sin \theta, \sin \alpha \sin \theta, \cos \theta)^T$. We use these plausible normals $\mathbf{n}_d, \mathbf{n}_{s1}, \mathbf{n}_{s2}$ as physical priors per pixel as input to the neural network.

Invertible Physical Model. The inverted physical model takes a rendered object surface normal map and derives the analytical polarimetric parameters, considering different reflection properties. The viewing angle θ_v is obtained from the dot product between the rendered surface normal map and the viewing vector \mathbf{v} . The analytical DoP $\hat{\rho}$ is derived for diffuse and specular reflection cases using Equation 2. This inverted physical model enables us to optimise the model using object shape cues, which is more robust in challenging lighting conditions compared to active depth sensors.

4. Polarimetric 6D Object Pose Estimation

Polarimetric images provide additional geometric information that improves the accuracy of 6D object pose prediction [9] (cf. Inputs in Fig.2). We explore its effectiveness in supervised training on real data and propose a self-supervised approach leveraging the analytical physical model, thus eliminating the need for annotated real data. Here, the supervised network is only pre-trained on synthetic data. The polarimetric real data is leveraged as self-supervision signal against the analytically derived polarimetric representation of the output of a differentiable renderer based on the predicted pose (cf. Fig.2).

Supervised Learning. The overall objective for the supervised learning is composed of both geometrical features learning and pose optimisation [9], as: $\mathcal{L} = \mathcal{L}_{pose} + \mathcal{L}_{geo}$, with: $\mathcal{L}_{pose} = \mathcal{L}_R + \mathcal{L}_{center} + \mathcal{L}_z$ and $\mathcal{L}_{geo} = \mathcal{L}_{mask} + \mathcal{L}_{normals} + \mathcal{L}_{xyz}$. Specifically, we employ separate loss terms for given ground truth rotation \mathbf{R} , (δ_x, δ_y) and δ_z as:

$$\begin{cases} \mathcal{L}_R &= \text{avg}_{\mathbf{x} \in \mathcal{M}} \|\mathbf{R}\mathbf{x} - \hat{\mathbf{R}}\mathbf{x}\|_1 \\ \mathcal{L}_{center} &= \|(\delta_x - \hat{\delta}_x, \delta_y - \hat{\delta}_y)\|_1, \\ \mathcal{L}_z &= \|\delta_z - \hat{\delta}_z\|_1 \end{cases} \quad (3)$$

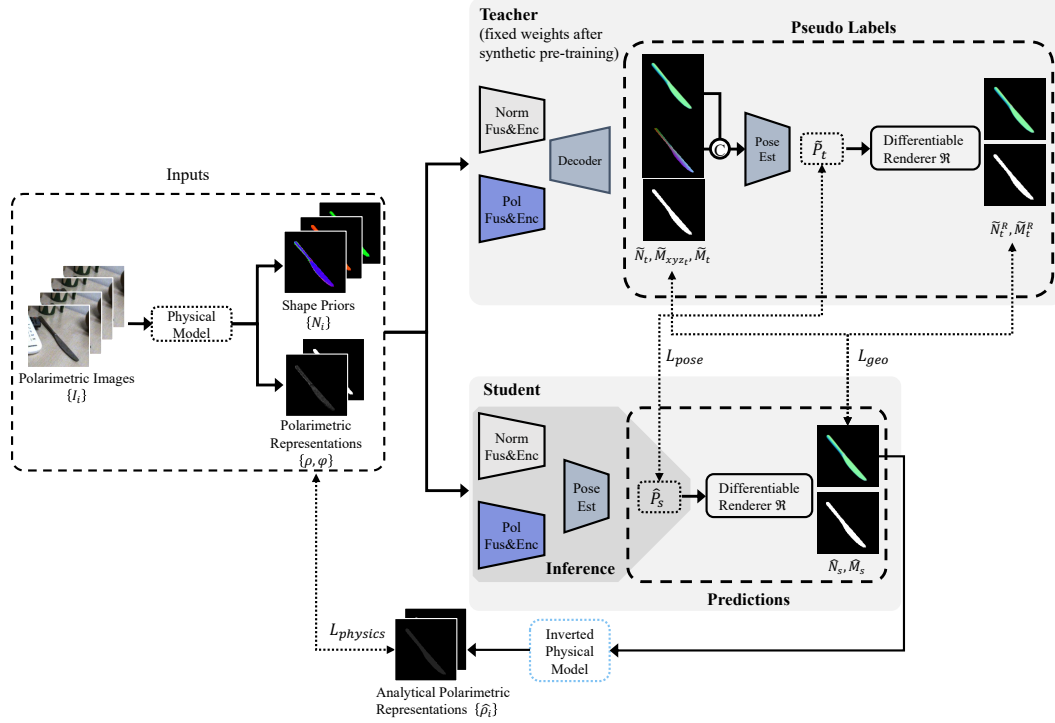


Figure 2. **Training Scheme Overview.** The upper branch, up until the pose estimation, is equivalent to the supervised training scheme. The training scheme utilises four polarisation images captured at different filter angles along with polarimetric and geometric representations derived from the physical model. The student network is optimised using pseudo labels (L_{pseudo}) generated by the teacher and by minimising the discrepancy between ρ from the physical model and $\hat{\rho}$ from the inverted physical model ($L_{physics}$). During inference, the lightweight student network predicts direct pose estimates (dark gray background).

Table 1. **Supervised Modalities Evaluation.** Impact of input-output modalities on supervised pose estimation (ADD).

Obj.	Photo. Chall.	Input Modalities				Outputs		Normal Metrics					Pose ADD
		RGB	Pol RGB	Phy. N	N	NOCS		mean↓	med↓	11.25°↑	22.5°↑	30°↑	
Cup		✓			✓	✓		-	-	-	-	-	91.1
			✓		✓	✓		7.3	5.5	86.2	96.1	97.9	91.3
			✓	✓	✓	✓		4.5	3.5	94.7	99.1	99.6	97.2
			✓		✓	✓		-	-	-	-	-	85.4
Fork	††	✓			✓	✓		-	-	-	-	-	86.1
			✓		✓	✓		11.0	7.3	72.6	90.7	93.9	92.9
			✓	✓	✓	✓		6.5	4.3	87.6	95.9	97.6	95.9
			✓		✓	✓		-	-	-	-	-	85.4

where $\hat{\bullet}$ denotes prediction. For symmetrical objects, the rotation loss is calculated based on the smallest loss from all possible ground-truth rotations under symmetry.

To learn the intermediate geometrical features, we employ additional losses with masks \mathbf{M} :

$$\begin{cases} \mathcal{L}_{mask} &= \|\mathbf{M} - \hat{\mathbf{M}}\|_1 \\ \mathcal{L}_{xyz} &= \mathbf{M} \odot \|\mathbf{M}_{xyz} - \hat{\mathbf{M}}_{xyz}\|_1 \\ \mathcal{L}_{normal} &= 1 - \langle \mathbf{n}, \hat{\mathbf{n}} \rangle \end{cases} \quad (4)$$

where \odot indicates the Hadamard product of element-wise multiplication, and $\langle \bullet, \bullet \rangle$ denotes the dot product.

Self-Supervised Learning. The self-supervised network (cf. Fig. 2) consists of a teacher network and a lightweight student network. Pre-trained on synthetic data, the networks

use pseudo-labels from the teacher to guide self-supervised learning of the student on real data. Our approach enhances and modifies established student-teacher training schemes for 6D object pose estimation [24], with detailed explanations and justifications in the following.

The teacher network (based on PPP-Net [9] as in the supervised scenario above) takes polarimetric intensities and shape priors as inputs. It predicts object mask $\tilde{\mathbf{M}}_t$, object normal map $\tilde{\mathbf{N}}_t$, and dense correspondences map $\tilde{\mathbf{M}}_{xyz_t}$. It estimates rotation and translation vectors to represent the pose as $\tilde{\mathbf{P}}_t = [\tilde{\mathbf{R}}_t \mid \tilde{\mathbf{t}}_t]$. The teacher network uses a differentiable renderer to generate pseudo labels, including object mask $\tilde{\mathbf{M}}_t^R$ and object normal map $\tilde{\mathbf{N}}_t^R$.

The lightweight student network directly predicts the pose $\hat{\mathbf{P}}_s$ without a geometric decoder. It is optimised using pseudo labels from the teacher network and generates

Table 2. **Supervised 6D Pose Benchmark comparisons.** We compare our method against recent RGB-D (FFB6D [12]) and RGB-only (GDR-Net [26]) methods on challenging objects with varying photometric conditions (\dagger) and depth map quality (good: + to low: -). We report the average recall of ADD(-S) for evaluation.

Object	Photo. Chall.	Refl.	Metal	Textureless	Transp.	Symm.	Depth Quality	RGB-D Split		RGB Split	
								FFB6D	Ours	GDR	Ours
Cup	\dagger	(*)					(+)	99.4	98.1	96.7	97.2
Teapot	\dagger	*	*				++	86.8	94.2	99.0	99.9
Can	\dagger	*	*				-	80.4	99.7	96.5	98.4
Fork	$\dagger\dagger$	*	*	*			--	37.0	72.4	86.6	95.9
Knife	$\dagger\dagger$	*	*	*			---	36.7	87.2	92.6	96.4
Bottle	$\dagger\dagger\dagger$	*		*	*	*	None	61.5	93.6	94.4	97.5
Mean								67.0	90.9	94.3	97.6

an object normal map $\hat{\mathbf{N}}_s$ and mask $\hat{\mathbf{M}}_s$ through rendering based on the predicted pose.

Our training scheme combines pseudo label learning and physics-induced self-supervision using polarimetric images. The pseudo label loss ($\mathcal{L}_{\text{pseudo}}$) transfers knowledge from the teacher network to the student network, while the physical loss term ($\mathcal{L}_{\text{physics}}$) optimizes the student’s prediction using raw polarisation data and the inverted physical model. These terms contribute to the overall loss (\mathcal{L}).

The pseudo label loss ($\mathcal{L}_{\text{pseudo}}$) is formulated as: $\mathcal{L}_{\text{pseudo}} = \lambda_1 \mathcal{L}_{\text{pose}} + \mathcal{L}_{\text{geo}}$, where $\mathcal{L}_{\text{pose}}$ measures the discrepancy between the predicted pose of the student network and the pseudo ground truth pose provided by the teacher network. The \mathcal{L}_{geo} term regularises the predicted mask and normal map by comparing them with the rendered mask and normal map. The weighting factor λ_1 depends on the alignment between the predicted shape and pose.

The physics-induced self-supervision loss ($\mathcal{L}_{\text{physics}}$) is formulated as: $\mathcal{L}_{\text{physics}} = \min_{\mathbf{x} \in \hat{\rho}_d, \hat{\rho}_s} |\rho - \mathbf{x}|$, where ρ is the ground truth degree of polarisation (DoP) obtained from real polarisation images, and $\hat{\rho}_d$ and $\hat{\rho}_s$ are the analytically computed diffuse and specular DoP using the inverted physical model. The loss term aligns the predicted DoP of the student network with the ground truth DoP. The overall loss is given by: $\mathcal{L} = \mathcal{L}_{\text{pseudo}} + \mathcal{L}_{\text{physics}}$.

5. Quantitative Results on Real Data

We conducted experiments to analyse the influence of input modality on pose estimation accuracy, specifically focusing on the impact of polarimetric image information. By comparing RGB-only and polar RGB inputs, we found that polarisation modality improves accuracy slightly, for the challenging object *fork*. Incorporating shape information from polarimetric images enhances pose estimation significantly, as evidenced by improved normals prediction and overall performance. These results highlight the network’s ability to establish a more accurate geometrical representation when guided by polarisation and shape cues (cf. Tab. 1).

Our experiments demonstrate the robustness of polarimetric imaging inputs in achieving accurate 6D pose prediction for photometrically challenging objects (cf. Tab. 2). Compared to FFB6D [12], which combines appearance and

Table 3. **Self-Supervised Quantitative Results.** Average recall of ADD(-S) metric is reported for different objects with increasing photometric complexity. \dagger as upper bound is identical to PPP-Net [9]; Self6D++ from [24]

Methods	Cup	Fork	Knife	Bottle	Mean
OURS _(Lower-Bound Student)	53.7	64.4	46.1	47.5	52.9
OURS _(Lower-Bound Teacher)	72.3	75.0	67.3	76.2	72.7
OURS _(Upper-Bound Student)	86.4	88.0	91.1	80.4	86.5
OURS _(Upper-Bound Teacher) \dagger	91.4	91.7	90.0	89.4	90.6
Self6D++	68.4	14.3	17.8	33.5	34.0
OURS_(RGB-Ps)	93.8	72.4	78.4	78.2	80.7

depth information, our method leverages polarimetric information to overcome challenges associated with photometric complexity, such as reflection or transparency.

Table 3 presents quantitative results that demonstrate the effectiveness of our self-supervision pipeline. We evaluate the performance of the teacher and student networks under different conditions. The OURS_(Lower-Bound Teacher) and OURS_(Lower-Bound Student) denote the lower bound performance when trained on synthetic data and tested on real data. The OURS_(Upper-Bound Teacher) and OURS_(Upper-Bound Student) represent the upper bound performance when trained and evaluated on real data using ground-truth labels, where the OURS_(Upper-Bound Teacher) is identical to PPP-Net [9]. Our model **OURS_(RGB-Ps)** consistently outperforms the SOTA RGB-D method [24] and achieves comparable results to the fully supervised upper bound baseline [9] for the *cup* object, which is the least complex in terms of photometric considerations.

6. Conclusion

Our proposed self-supervised framework leveraging polarimetric information has demonstrated its effectiveness in improving 6D object pose estimation accuracy. By integrating pseudo label learning and physics-induced self-supervision, our approach achieves superior performance compared to existing RGB-D methods and even approaches the results of fully supervised methods. The utilisation of polarimetric images as additional inputs provides valuable complementary information and helps bridging the domain gap between synthetic and real data. These findings highlight the potential of self-supervision and polarimetric imaging in advancing the field of object pose estimation.

References

- [1] Gary A Atkinson. Polarisation photometric stereo. *Computer Vision and Image Understanding*, 160:158–167, 2017.
- [2] Gary A Atkinson and Edwin R Hancock. Multi-view surface reconstruction using polarization. In *Tenth IEEE International Conference on Computer Vision (ICCV’05) Volume 1*, volume 1, pages 309–316. IEEE, 2005.
- [3] Gary A Atkinson and Edwin R Hancock. Recovery of surface orientation from diffuse polarization. *IEEE transactions on image processing*, 15(6):1653–1664, 2006.
- [4] Yunhao Ba, Alex Gilbert, Franklin Wang, Jinfa Yang, Rui Chen, Yiqin Wang, Lei Yan, Boxin Shi, and Achuta Kadambi. Deep shape from polarization. In *Computer Vision–ECCV 2020: 16th European Conference, Glasgow, UK, August 23–28, 2020, Proceedings, Part XXIV 16*, pages 554–571. Springer, 2020.
- [5] Tuo Cao, Fei Luo, Yanping Fu, Wenxiao Zhang, Shengjie Zheng, and Chunxia Xiao. Dgecn: A depth-guided edge convolutional network for end-to-end 6d pose estimation. *arXiv preprint arXiv:2204.09983*, 2022.
- [6] Zhaopeng Cui, Jinwei Gu, Boxin Shi, Ping Tan, and Jan Kautz. Polarimetric multi-view stereo. In *Proceedings of the IEEE Conference on Computer Vision and Pattern Recognition*, pages 1558–1567, 2017.
- [7] Yan Di, Fabian Manhardt, Gu Wang, Xiangyang Ji, Nassir Navab, and Federico Tombari. So-pose: Exploiting self-occlusion for direct 6d pose estimation. In *Proceedings of the IEEE/CVF International Conference on Computer Vision*, pages 12396–12405, 2021.
- [8] Torsten Fließbach. *Elektrodynamik: Lehrbuch zur Theoretischen Physik II*, volume 2. Springer-Verlag, 2012.
- [9] Daoyi Gao, Yitong Li, Patrick Ruhkamp, Iuliia Skobleva, Magdalena Wysock, HyunJun Jung, Pengyuan Wang, Arturo Guridi, Nassir Navab, and Benjamin Busam. Polarimetric pose prediction. In *Proceedings of the European Conference on Computer Vision (ECCV)*, 2022.
- [10] Daoyi Gao, Patrick Ruhkamp, Nassir Navab, and Benjamin Busam. S2p3 - self-supervised polarimetric pose prediction. *Under Review*, 2023.
- [11] N Missael Garcia, Ignacio De Erausquin, Christopher Edmiston, and Viktor Gruev. Surface normal reconstruction using circularly polarized light. *Optics express*, 23(11):14391–14406, 2015.
- [12] Yisheng He, Haibin Huang, Haoqiang Fan, Qifeng Chen, and Jian Sun. Ffb6d: A full flow bidirectional fusion network for 6d pose estimation. In *IEEE/CVF Conference on Computer Vision and Pattern Recognition (CVPR)*, June 2021.
- [13] Tomas Hodan, Daniel Barath, and Jiri Matas. Epos: Estimating 6d pose of objects with symmetries. In *Proceedings of the IEEE/CVF conference on computer vision and pattern recognition*, pages 11703–11712, 2020.
- [14] Xiaoke Jiang, Donghai Li, Hao Chen, Ye Zheng, Rui Zhao, and Liwei Wu. Uni6d: A unified cnn framework without projection breakdown for 6d pose estimation. *arXiv preprint arXiv:2203.14531*, 2022.
- [15] HyunJun Jung, Shun-Cheng Wu, Patrick Ruhkamp, Hannah Schieber, Pengyuan Wang, Giulia Rizzoli, Hongcheng Zhao, Sven Damian Meier, Daniel Roth, Nassir Navab, et al. Housecat6d—a large-scale multi-modal category level 6d object pose dataset with household objects in realistic scenarios. *arXiv preprint arXiv:2212.10428*, 2022.
- [16] Achuta Kadambi, Vage Taamazyan, Boxin Shi, and Ramesh Raskar. Depth sensing using geometrically constrained polarization normals. *International Journal of Computer Vision*, 125(1-3):34–51, 2017.
- [17] Zhigang Li, Gu Wang, and Xiangyang Ji. Cdpn: Coordinates-based disentangled pose network for real-time rgb-based 6-dof object pose estimation. In *Proceedings of the IEEE/CVF International Conference on Computer Vision*, pages 7678–7687, 2019.
- [18] Ningkai Mo, Wanshui Gan, Naoto Yokoya, and Shifeng Chen. Es6d: A computation efficient and symmetry-aware 6d pose regression framework. *arXiv preprint arXiv:2204.01080*, 2022.
- [19] Kiru Park, Timothy Patten, and Markus Vincze. Pix2pose: Pixel-wise coordinate regression of objects for 6d pose estimation. In *Proceedings of the IEEE/CVF International Conference on Computer Vision*, pages 7668–7677, 2019.
- [20] Ivan Shugurov, Fu Li, Benjamin Busam, and Slobodan Ilic. Osop: A multi-stage one shot object pose estimation framework. *arXiv preprint arXiv:2203.15533*, 2022.
- [21] Ivan Shugurov, Sergey Zakharov, and Slobodan Ilic. Dpodv2: Dense correspondence-based 6 dof pose estimation. *IEEE Transactions on Pattern Analysis and Machine Intelligence*, 2021.
- [22] William AP Smith, Ravi Ramamoorthi, and Silvia Tozza. Height-from-polarisation with unknown lighting or albedo. *IEEE transactions on pattern analysis and machine intelligence*, 41(12):2875–2888, 2018.
- [23] Yongzhi Su, Mahdi Saleh, Torben Fetzter, Jason Rambach, Nassir Navab, Benjamin Busam, Didier Stricker, and Federico Tombari. Zebrapose: Coarse to fine surface encoding for 6dof object pose estimation. *arXiv preprint arXiv:2203.09418*, 2022.
- [24] Gu Wang, Fabian Manhardt, Xingyu Liu, Xiangyang Ji, and Federico Tombari. Occlusion-aware self-supervised monocular 6d object pose estimation. *IEEE Transactions on Pattern Analysis and Machine Intelligence*, 2021.
- [25] Gu Wang, Fabian Manhardt, Jianzhun Shao, Xiangyang Ji, Nassir Navab, and Federico Tombari. Self6d: Self-supervised monocular 6d object pose estimation. In *European Conference on Computer Vision*, pages 108–125. Springer, 2020.
- [26] Gu Wang, Fabian Manhardt, Federico Tombari, and Xiangyang Ji. Gdr-net: Geometry-guided direct regression network for monocular 6d object pose estimation. In *Proceedings of the IEEE/CVF Conference on Computer Vision and Pattern Recognition*, pages 16611–16621, 2021.
- [27] Pengyuan Wang, HyunJun Jung, Yitong Li, Siyuan Shen, Rahul Parthasarathy Srikanth, Loranzo Garattoni, Sven Meier, Nassir Navab, and Benjamin Busam. Phocal: A multimodal dataset for category-level object pose estimation with photometrically challenging objects. In *IEEE/CVF Conference on Computer Vision and Pattern Recognition (CVPR)*. IEEE, 2022.

- [28] He Yisheng, Wang Yao, Fan Haoqiang, Chen Qifeng, and Sun Jian. Fs6d: Few-shot 6d pose estimation of novel objects. *CVPR*, 2022.
- [29] Ye Yu, Dizhong Zhu, and William AP Smith. Shape-from-polarisation: a nonlinear least squares approach. In *Proceedings of the IEEE International Conference on Computer Vision Workshops*, pages 2969–2976, 2017.
- [30] Sergey Zakharov, Ivan Shugurov, and Slobodan Ilic. Dpod: 6d pose object detector and refiner. In *Proceedings of the IEEE/CVF International Conference on Computer Vision*, pages 1941–1950, 2019.
- [31] Dizhong Zhu and William AP Smith. Depth from a polarisation + rgb stereo pair. In *Proceedings of the IEEE/CVF Conference on Computer Vision and Pattern Recognition*, pages 7586–7595, 2019.